CHEMISTRY
A EUROPEAN JOURNAL

DOI: 10.1002/chem.201001259

Enhancing the Blocking Temperature in Single-Molecule Magnets by Incorporating 3d–5d Exchange Interactions

Kasper S. Pedersen,*[a] Magnus Schau-Magnussen,[a] Jesper Bendix,*[a] Høgni Weihe,[a] Andrei V. Palii,[b] Sophia I. Klokishner,[b] Serghei Ostrovsky,[b] Oleg S. Reu,[b] Hannu Mutka,[c] and Philip L. W. Tregenna-Piggott†[d]

Dedicated to the memory of Dr. Philip L. W. Tregenna-Piggott

Abstract: We report the first single-molecule magnet (SMM) to incorporate the $[Os(CN)_6]^{3-}$ moiety. The compound (**1**) has a trimeric, cyanide-bridged Mn^{III}-Os^{III}-Mn^{III} skeleton in which Mn^{III} designates a [Mn(5-Brsalen)(MeOH)]$^+$ unit (5-Brsalen = *N*,*N*′-ethylenebis(5-bromosalicylideneiminato)). X-ray crystallographic experiments reveal that **1** is isostructural with the Mn^{III}-Fe^{III}-Mn^{III} analogue (**2**). Both compounds exhibit a frequency-dependent out-of-phase $\chi''(T)$ alternating current (ac) susceptibility signal that is suggestive of SMM behaviour. From the Arrhenius expression, the effective barrier for **1** is found to be $\Delta_{eff}/k_B = 19$ K ($\tau_0 = 5.0\times10^{-7}$ s; k_B = Boltzmann constant), whereas only the onset (1.5 kHz, 1.8 K) of $\chi''(T)$ is observed for **2**, thus indicating a higher blocking temperature for **1**. The strong spin–orbit coupling present in Os^{III} isolates the $E'_{1g(1/2)}(O_h^*)$ Kramers doublet that exhibits orbital contributions to the single-ion anisotropy. Magnetic susceptibility and inelastic neutron-scattering measurements reveal that substitution of $[Fe(CN)_6]^{3-}$ by the $[Os(CN)_6]^{3-}$ anion results in larger ferromagnetic, anisotropic exchange interactions going from quasi-Ising exchange interactions in **2** to pure Ising exchange for **1** with $J_{\parallel}^{MnOs} = -30.6$ cm^{-1}. The combination of diffuse magnetic orbitals and the Ising-type exchange interaction effectively contributes to a higher blocking temperature. This result is in accordance with theoretical predictions and paves the way for the design of a new generation of SMMs with enhanced SMM properties.

Keywords: anisotropy · magnetic properties · manganese · osmium · single-molecule magnets

Introduction

Future prospects for designing molecular magnetic materials with properties such as tuneable blocking temperatures rely fundamentally on the understanding of microscopic orbital interactions between the paramagnetic building blocks. Whereas the effect of incorporating 3d transition-metal ions with various electron configurations is more or less well-established, that of substituting 3d metal ions with 4d or 5d metal ions is far less explored. Experimental evidence for enhanced magnetic interactions in compounds that utilise metal ions with more diffuse orbitals was first observed by Girolami and Entley in 1995[1] in their study of a vanadium(III)-containing Prussian Blue analogue. The theoretical interpretation was founded on significant delocalisation of 3d electron density to bridging cyanide π* orbitals that favour strong magnetic superexchange. Within the field of molecular magnetism, single-molecule magnets (SMMs)[2,3] have attracted considerable interest in recent years due to

[a] K. S. Pedersen, M. Schau-Magnussen, Prof. J. Bendix, Dr. H. Weihe
Department of Chemistry, University of Copenhagen
Universitetsparken 5, 2100 Copenhagen (Denmark)
Fax: (+45) 35-32-02-12
E-mail: ksp@kiku.dk
bendix@kiku.dk

[b] Dr. A. V. Palii, Prof. S. I. Klokishner, Dr. S. Ostrovsky, Dr. O. S. Reu
Institute of Applied Physics, Academy of Sciences of Moldova
Academy str. 5, 2028 Kishinev (Moldova)

[c] Dr. H. Mutka
Institut Laue-Langevin, 6 Rue Jules Horowitz
BP-156-38042 Grenoble Cedex 9 (France)

[d] Dr. P. L. W. Tregenna-Piggott
Paul Scherrer Institute
5232 Villigen PSI (Switzerland)

[†] Deceased.

Supporting information for this article is available on the WWW under http://dx.doi.org/10.1002/chem.201001259.

the possible application of such molecules in high-density data storage, quantum computing and molecular spintronics.[4] SMMs differ fundamentally from traditional magnetic materials as the magnetism is a purely intrinsic property of the isolated molecule. The origin of the anisotropy barrier (Δ) in the majority of SMMs so far prepared is dictated by the molecule ground-state spin (S_T) and the easy-axis zero-field-splitting (ZFS) parameter (D): $\Delta = |D|S_T^2$ (for integer spin). These SMMs are clusters formed from transition-metal ions in which the orbital angular momentum has been largely quenched by the ligand field. The magnetic exchange is dominated by Heisenberg exchange interactions and the global uniaxial anisotropy can be expressed through single-ion contributions from the constituent centres. Despite the voluminous work in the area, discoveries of SMMs with blocking temperature comparable to the prototype Mn_{12} have been few and far between. This may be attributed to two factors. First, the zero-field splittings of the constituent ions are essentially a second-order effect, typically on the order of a few wavenumbers. Secondly, the contribution of these single-ion anisotropies to the overall uniaxial anisotropy of the cluster decreases with increasing S, such that Δ does not increase with S^2 but as S^0.[5]

One approach of increasing interest is to incorporate metal ions with first-order orbital angular momentum, as this strategy has the potential to increase the barrier for magnetisation reversal, thereby benefiting both from the strong (first-order) single-ion anisotropy and anisotropic orbitally dependent exchange interactions. Three distinct approaches have been pursued to achieve this aim. The first is the introduction of 3d metal ions with unquenched orbital angular momenta.[6] It was argued that under certain conditions the axial local crystal field in combination with the spin–orbit interaction introduces a significant splitting of the m_j levels. At low temperature, the systems can often be described by the effective pseudo-spin-$^1/_2$ Hamiltonian that involves only the ground doublets (effective spin $^1/_2$) for the orbitally degenerate ions and true spins for the pure spin ions. In some cases, the overall anisotropy that arises from both local and exchange anisotropic contributions can create the barrier needed for the magnetisation reversal characteristic of SMM behaviour.[7–10] The important feature of these systems that sets them apart from conventional spin clusters is that the barrier height proves to be dependent on the strength of the exchange interaction.

The second approach is the introduction of lanthanide metal ions. Benefiting from the high anisotropy of the 4f ions in axial crystal fields, this approach opened a new trend in the design of SMMs, with high blocking temperatures achieved for mononuclear lanthanide complexes.[11–16] A qualitatively different situation takes place in mixed 3d/4f compounds when the symmetry of the ligand surroundings of the lanthanide ions is lower than axial. The exchange interaction, though small, plays an important role in suppressing the transverse anisotropy, as exemplified by the recently reported tetrameric Cu_2Tb_2 cluster.[17,18]

The third approach that is far less explored consists of replacing 3d transition metal ions with 4d or 5d ones. This substitution leads to two important consequences: 1) The spin–orbit interaction in 4d and 5d ions is at least one order of magnitude larger than for 3d ions, thus resulting in the ground doublet being more isolated from the excited levels. For this reason, the conditions for the applicability of the pseudo-spin-$^1/_2$ Hamiltonian in this case are much better. 2) The exchange interaction is much stronger than in the case of 3d ions, and this interaction is usually highly anisotropic (Ising or quasi-Ising) due to the orbitally dependent contributions to the magnetic superexchange. Therefore one can expect that the magnetisation reversal barrier can be significantly increased compared to clusters of 3d ions. Despite the prospect of stronger magnetic interactions,[19] SMMs that incorporate heavier transition metals are limited to a few SMMs based on homo- and heteroleptic cyano complexes of rhenium,[20–23] tungsten[24,25] and molybdenum.[26] Notably, Long and co-workers reported that replacing chromium with molybdenum in $[(Me_3tacn)_6Mn^{II}Cr^{III}{}_6(CN)_{18}]^{2+}$ ($Me_3tacn = N,N',N''$-trimethyl-1,4,7-triazacyclononane) furnishes an SMM.[26]

SMMs that incorporate the heavier Group 8 metals have yet to be reported, even though both $[Ru(CN)_6]^{3-}$[19] and $[Os(CN)_6]^{3-}$[27] are well described in the literature. Since $[Ru(CN)_6]^{3-}$ is readily reduced to $[Ru(CN)_6]^{4-}$ and is not stable in solution, syntheses that involve organic ligands are often not possible. However, the recently structurally characterised Os^{III}[27] counterpart is more stable and hence more comfortably incorporated into clusters with organic co-ligands. In a paper devoted to hypothetical clusters that incorporate the $[Os(CN)_6]^{3-}$ anion, Mironov[28] argued that the exchange coupling in linear Os-CN-M groups should be strongly anisotropic due to orbital contributions to the kinetic exchange. Parallel to the work reported in this paper, the first cyanide-bridged materials based on the hexacyanoosmate(III) anion were reported by Dunbar's group in the form of the pentanuclear complexes $[\{Ni(tmphen)_2\}_3\{Os(CN)_6\}_2]\cdot 6MeCN$[29] (tmphen = 3,4,7,8-tetramethyl-1,10-phenanthroline) and $[\{Fe(tmphen)_2\}_3\{Os(CN)_6\}_2]\cdot 9H_2O$.[30] Although the former cluster was shown to exhibit magnetic anisotropy, the sign of this anisotropy is incompatible with SMM behaviour.[31] As to the use of other 3d ions instead of Ni, theoretical considerations suggest that the magnetisation reversal barriers for the hypothetical trigonal bipyramidal $Os^{III}{}_2Cr^{II}{}_3$ and $Os^{III}{}_2Mn^{II}{}_3$ clusters are unlikely to be pronounced.[28] The different orientation of the local anisotropy axes of the exchange-coupled Os-CN-M pairs in trigonal bipyramidal structures does not take full advantage of the strong anisotropy of the orbitally dependent superexchange. From this point of view, the synthesis of linear clusters that comprise orbitally degenerate 4d and 5d ions seems to be more promising because all local anisotropy axes are aligned parallel and the global anisotropy is expected to be maximal.

This situation is encountered in the class of polynuclear compounds that contain two high-spin Mn^{III} Schiff base

units bridged by a $[M^{III}(CN)_6]^{3-}$ anion, K[{Mn(5-Brsalen)-(H_2O)}$_2$$M^{III}(CN)_6$]·2$H_2O$ (5-Brsalen = *N*,*N*′-ethylenebis(5-bromosalicylideneiminato)), which has been known for about a decade.[32,33] The compounds formed with M^{III} = Co, Fe and Cr are all isostructural and SMM behaviour was recently suggested for the Cr and Fe compounds.[34] Another related trimer is $(NEt_4)[Mn_2(rac\text{-salmen})_2(MeOH)_2Fe(CN)_6]$ (*rac*-salmen^{2-} = *rac*-*N*,*N*′-(1-methylethylene)bis(salicylideneiminate)) reported by Ferbinteanu et al., which exhibits an enhanced effective barrier of $\Delta_{eff}/k_B = 14$ K (k_B = Boltzmann constant).[35] Because of the relatively simple geometry and small number of constituent metal ions, the modelling of these compounds is relatively simple and involves only few parameters.

We report the synthesis, structure and magnetic properties of $(NEt_4)[Mn_2(5\text{-Brsalen})_2(MeOH)_2M(CN)_6]$ with M = Os (**1**) and Fe (**2**). Probing the electronic structure by both magnetic susceptibility and inelastic neutron-scattering experiments leads to a very precise definition of the intra- and intermolecular interactions. In particular, we demonstrate that **1** exhibits enhanced magnetic interactions over analogous **2** and identify the challenges that will have to be faced for the blocking temperature in this class of compounds to be increased further.

Results

Single-crystal X-ray diffraction experiments reveal that **1** (Figure 1) and **2** are isostructural and crystallise in the monoclinic space group $P2_1/c$. Each trimeric molecule consists of two $[Mn^{III}(5\text{-Brsalen})]^+$ units bridged by *trans* coordination of an $[M(CN)_6]^{3-}$ unit. The overall charge is compensated by systematically disordered NEt_4^+ counterions and the sixth coordination site of Mn^{III} is occupied by a methanol molecule that is engaged in hydrogen bonding to a neighbouring molecule. The central Os^{III} resides in a nearly octahedral environment with *cis* C-Os-C angles of (90 ± 2.58)° and Os–C bond lengths of 2.048–2.063 Å. $d(C\text{–}N)_{CN^-}$ are in the range of 1.148–1.162 Å, for which the longer are involved in Mn bridging or hydrogen bonding. Crystallographic data for compounds **1** and **2** can be found in Table 1.

Table 1. Crystallographic data for **1** and **2**.

	1	**2**
formula	$C_{48}H_{52}Br_4Mn_2N_{11}O_6Os$	$C_{48}H_{52}Br_4FeMn_2N_{11}O_6$
M_r	1498.73	1364.38
colour, shape	brown, prism	brown, prism
crystal size [mm^3]	0.25 × 0.14 × 0.1	0.3 × 0.23 × 0.09
crystal system	monoclinic	monoclinic
space group	$P2_1/c$ (no. 14)	$P2_1/c$ (no. 14)
T [K]	122 (1)	122 (1)
a [Å]	12.2962 (12)	12.3100 (18)
b [Å]	15.5503 (16)	15.4346 (16)
c [Å]	15.699 (2)	15.542 (1)
β [°]	115.44 (13)	114.68 (1)
V [Å^3]	2710.7 (5)	2683.3 (5)
Z	2	2
ρ_{calcd} [g cm^{-3}]	1.836	1.689
$F(000)$	1462	1362
$\mu(Mo_{K\alpha})$ [mm^{-1}]	5.80	3.77
θ range [°]	1.8–35.1	1.8–30.1
collected reflns	86222	66211
unique reflns	11991	7852
parameters/restraints	350/1	350/1
reflections ($I > 2\sigma(I)$)	9448	6237
GOF	1.12	1.14
$R1$[a] ($I > 2\sigma(I)$)	0.030	0.028
$R1$[a] (all data)	0.053	0.049
$wR2$[b] (all data)	0.080	0.077
max/min $\Delta\rho$ [e Å^{-3}]	1.12/−1.70	0.83/−1.09

[a] $R1 = \Sigma||F_o| - |F_c||/\Sigma|F_o|$. [b] $wR2 = [\Sigma w(F_o^2 - F_c^2)^2/\Sigma w(F_o^2)^2]^{1/2}$

The $[Os(CN)_6]^{3-}$ anion is subject to a strong cubic ligand field that gives rise to a $^2T_{2g}$ (O_h) ground term, split by spin–orbit coupling ($\zeta_{Os^{III}} \approx 3000$ cm^{-1})[27] into the states $E'_{1g(1/2)}$ and $G'_{g(3/2)}$ of the double group O_h*, with the Kramers doublet $E'_{1g(1/2)}$ ($m_j = \pm 1/2$) lower lying, as depicted in Figure 2.

It is straightforward to show[36] that the effective ground-state g factor is given by the following Equation (1):

$$g_{eff}(Os) = \frac{1}{3}(g_e + 4\kappa) \quad (1)$$

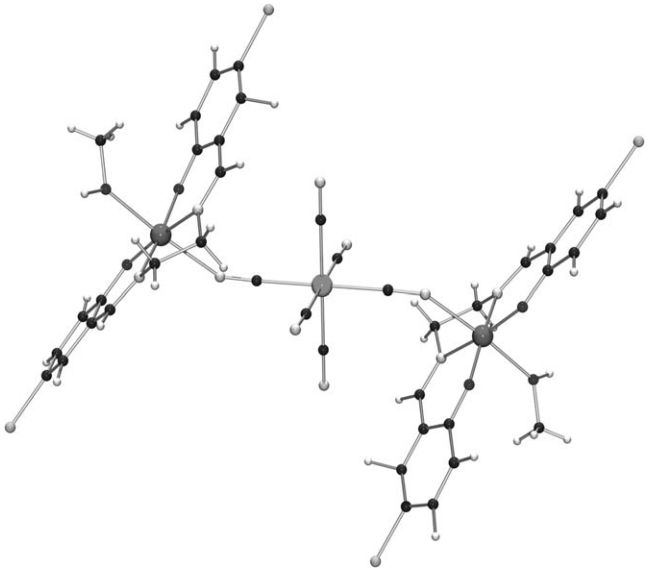

Figure 1. X-ray structure of **1**. The NEt_4^+ counterions are not shown.

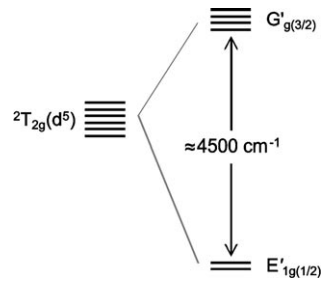

Figure 2. Splitting of the $^2T_{2g}$ ground term by spin–orbit coupling.

in which g_e is the electronic g factor and κ is the orbital reduction factor; for $\kappa = 0.85$, $g_{eff} \approx 1.8$. The splitting of the $^2T_{2g}$ (O_h) ground term by the low-symmetry components of the ligand field is expected to be much smaller than that of spin–orbit coupling. The magnetic moment of the Os^{III} anion may then be represented by a pseudo-spin-$^1/_2$ operator over the complete experimental temperature range, with g factors approximating to Equation (1). The two Mn^{III} ions are represented by the true spin-2 operators. To second-order, the zero-field splitting of the $s = 2$ states is given by Equation (2):

$$\hat{H}_{ZFS} = D_{Mn}\left(\hat{s}_z^2 - \frac{1}{3}s(s+1)\right) + E_{Mn}(\hat{s}_x^2 - \hat{s}_y^2) \quad (2)$$

in which D_{Mn} and E_{Mn} are axial and rhombic zero-field-splitting parameters. From previous studies of similar trimeric molecules, the ZFS (D_{Mn}) of the Mn^{III} centres was found to be in the range of -3.5 to $-4.0\ cm^{-1}$ and large deviations from these values for **1** are not to be expected. Imposing axial symmetry on the osmium(III)–manganese(III) exchange interaction, the Hamiltonian has the following form [Eq. (3)]:

$$\hat{H}_{ex}(Os - Mn) = J_{\parallel}\hat{\tau}_z(Os)\hat{s}_z(Mn) + J_{\perp}[\hat{\tau}_x(Os)\hat{s}_x(Mn) + \hat{\tau}_y(Os)\hat{s}_y(Mn)] \quad (3)$$

in which $\hat{\tau}_z(Os)$, $\hat{\tau}_x(Os)$ and $\hat{\tau}_y(Os)$ are the components of the pseudo-spin-$^1/_2$ operator that describes the ground Kramers doublet of the Os^{III} ion, and $\hat{s}_z(Mn)$, $\hat{s}_x(Mn)$ and $\hat{s}_y(Mn)$ denote the components of the spin operators of the Mn^{III} ion ($s = 2$). Note that the Os-CN-Mn group is not linear and, furthermore, there is no group-theoretical grounds for the coincidence of the z axis of the Mn^{III} ZFS tensor with the unique axis of anisotropic exchange interaction. Nevertheless, the easy axis of the manganese(III) centre is also expected to be closely aligned with the long Mn–NC bond that defines the Jahn–Teller distortion of the manganese(III) complex and adequate agreement with experiment could be obtained without the need for a further coordinate transformation. The Hamiltonian of the whole system looks as follows [Eq. (4)]:

$$\hat{H} = \sum_{i=Mn_1,\,Mn_2}\left\{D_{Mn}\left[\hat{s}_Z^2(i) - {}^1/_3 s(s+1)\right] + E_{Mn}(\hat{s}_X^2(i) - \hat{s}_Y^2(i)) + J_{\parallel}{}^{MnOs}\hat{\tau}_z(Os)\hat{s}_z(i) + J_{\perp}{}^{MnOs}\left[\hat{\tau}_x(Os)\hat{s}_x(i) + \hat{\tau}_Y(Os)\hat{s}_Y(i)\right] + \mu_B g_{Mn}\mathbf{B}\hat{\mathbf{s}}(i)\right\} + J_{MnMn}\hat{\mathbf{s}}(Mn_1)\hat{\mathbf{s}}(Mn_2) + \mu_B g_{eff}(Os)\mathbf{B}\hat{\boldsymbol{\tau}}(Os) \quad (4)$$

The spectroscopic and magnetic data were all calculated with the aid of the eigenvalues and eigenfunctions of this Hamiltonian. J_{MnMn} is the parameter of the isotropic exchange between the Mn^{III} ions and the g values are approximated to be isotropic fixed at $g_{Mn} = 1.98$ and $g_{eff}(Os) = 1.8$. An inter-cluster interaction is included by calculating the principal components of the susceptibility as $(\chi_{x,y,z})^{-1} = \left(\chi_{x,y,z}^{mol}\right)^{-1} - \lambda$ in which $\chi_{x,y,z}^{mol}$ is the susceptibility calculated by utilising the Hamiltonian in Equation (4) and λ is the molecular-field constant. The powder susceptibility was calculated by averaging the three principal components. This procedure is strictly applicable at temperatures well above the ordering temperature but was found to be nearly equivalent to the more rigorous self-consistent field method described earlier,[34] for the small values of λ identified, in the 11–300 K temperature range. Further details of the methods employed to calculate the inelastic neutron scattering (INS) spectra and magnetic susceptibility may be found in the Supporting Information and ref. [34].

The variation of the magnetic susceptibility with temperature is shown in Figure 3. The value of χT rises gradually upon cooling from 300 K to around 25 K, which is suggestive of a ferromagnetic interaction between the manganese(III) and osmium(III) cations, and then falls precipitously upon cooling further to 2 K, indicative of antiferromagnetic exchange interactions between the trimers. The high-temperature value of $6.3\ cm^3\,K\,mol^{-1}$ of the χT product is in excellent agreement with the calculated value for the uncorrelated two Mn^{III} ions ($s = 2$, $g = 1.98$) and one Os^{III} ion ($\tau = {}^1/_2$, $g_{eff}(Os) = 1.8$).

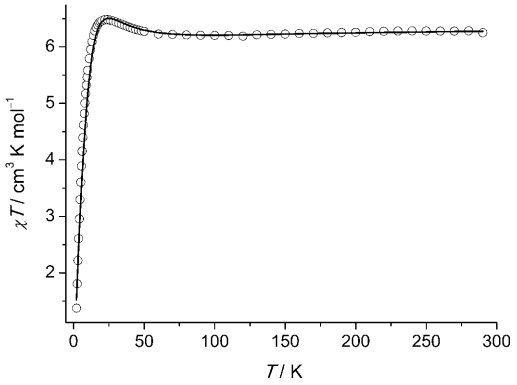

Figure 3. Variation of χT versus T, measured and calculated for **1**. The theoretical model was calculated with the parameters $g_{Mn} = 1.98$, $g_{eff}(Os) = 1.8$, $D_{Mn} = -4.3\ cm^{-1}$, $E_{Mn}/D_{Mn} = 0.057$, $J_{MnMn} = +3.2\ cm^{-1}$, $J_{\parallel}^{MnOs} = -30.6\ cm^{-1}$, $J_{\perp}^{MnOs} = 0\ cm^{-1}$ and $\lambda = -0.44\ cm^{-3}$ mol.

The INS spectrum recorded at 1.5 K with an incident neutron wavelength of 3.8 Å (Figure 4, top) exhibits two peaks located at around 15.3 and around 28.3 cm^{-1}, which are assigned to magnetic excitations based on the Q dependencies of the intensities. On warming to 15 K, two energy-gain transitions are observed at 8 and 15 cm^{-1} together with two low-intensity hot transitions at 18 and 23 cm^{-1}. The INS transition energies and magnetic susceptibility data were refined concomitantly to the model Hamiltonian using the program MagProp[37] and the theoretical INS spectrum was

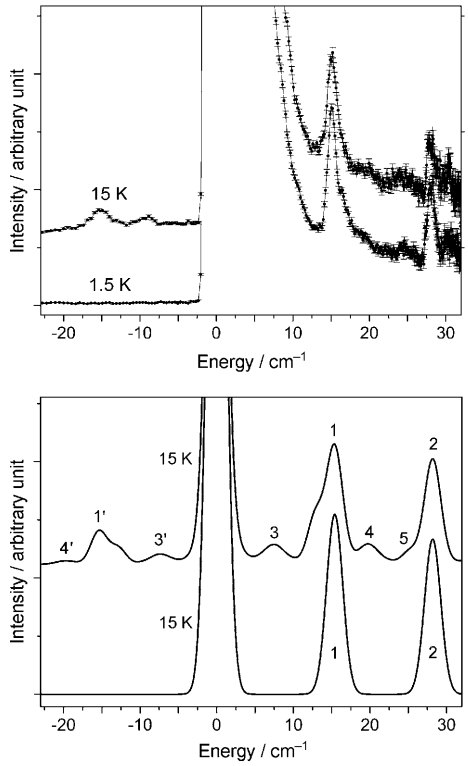

Figure 4. INS spectrum of **1** obtained with an incident neutron wavelength of 3.8 Å (top) and theoretical INS spectrum (bottom) calculated by means of the parameters given in the caption of Figure 3.

calculated using the program INS.[38] The model curves are shown as solid lines in Figure 4 (bottom) and are in good agreement with experiment, thereby providing confidence in the parameters derived. SMM behaviour is suggested in both **1** and **2** (Figure 5 and the Supporting Information for **2**) from the frequency dependency of the in-phase ($\chi'(T)$) and out-of-phase ($\chi''(T)$) alternating current (ac) signal. However, no maximum in $\chi''(T)$ is observed for **2** with the accessible frequency range (1–1500 Hz), thus indicating a low barrier for spin reversal. Estimating the relaxation times

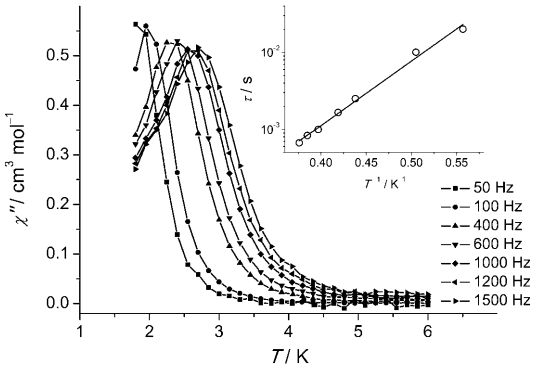

Figure 5. Temperature dependency of the out-of-phase component of the molar ac magnetic susceptibility for **1** measured in a 3 Oe field oscillating at selected frequencies. The inset shows the Arrhenius plot.

for **1** from the peak positions yields a linear relation in accordance with the Arrhenius expression ($\ln\{\tau(T)\} = \ln(\tau_0) + \Delta_{eff}/(k_B T)$) from which the parameters $\Delta_{eff}/k_B = 19$ K and $\tau_0 = 5.0 \times 10^{-7}$ s could be extracted.

Discussion

The spin-Hamiltonian parameters given in the caption of Figure 3 for **1** (for **2**, see the Supporting Information) show the ZFS parameters for Mn^{III} to be close to those found for similar Mn-Fe-Mn, Mn-Cr-Mn and Mn-Co-Mn trimers.[34] Likewise, a satisfactory account of the **2** data could be obtained with J_{MnMn} set to zero, whereas this parameter takes the value of $+3.2$ cm^{-1} in the refinement of the data for **1**. The outstanding difference in the microscopic magnetic interactions between **1** and **2**, follows from the difference between Mn^{III}–Fe^{III} and Mn^{III}–Os^{III} exchange couplings. For a closely related Mn-Co-Mn trimer that contains diamagnetic Co^{III}, a J_{MnMn} of $+0.63$ cm^{-1} was found and the larger value for **1** is expected due to the more diffuse 5d orbitals.[34] The data for **1** and **2** were refined the same way with the same Hamiltonian to yield $J_{\parallel}^{MnFe} = -5.8$ cm^{-1}, $J_{\perp}^{MnFe} = -3.2$ cm^{-1}, $J_{\parallel}^{MnOs} = -30.6$ cm^{-1} and $J_{\perp}^{MnOs} \approx 0$ cm^{-1}. These are the best fit values obtained from a range of different starting guesses for the fitted parameters including both positive and negative and isotropic as well as anisotropic values for $J_{\parallel}^{MnOs}$ and $J_{\perp}^{MnOs}$. Details of the fitting procedure are given in the Supporting Information. The increase in the magnitude of the exchange coupling upon descending the iron group is expected. The key point is the dramatic change from a quasi-isotropic ferromagnetic interaction to one that is of Ising-type. The fundamental reason for this is the larger spin–orbit coupling of Os^{III} compared to Fe^{III}, which gives rise to a ground state with unquenched orbital angular momentum. The orbitally dependent exchange coupling terms then give rise to the profound anisotropy.

The spin-relaxation barrier for **1** is $\Delta_{eff}/k_B = 19$ K, but in contrast the out-of-phase component of the susceptibility of **2** displays but the onset of peaks upon cooling to around 1.8 K, thus indicating a low relaxation barrier. The relaxation barrier for trimers based on Mn-Os-Mn units could, however, be far larger. For clusters formed from 3d transition metals with orbitally non-degenerate ground terms, there exists a good correlation between the spin-reversal barrier, determined from ac susceptibility measurements, and the energy gap between the ground-state doublet and the states of the doublet differing by one in the quantum number M_S.[39] This is because the direct absorption of phonons can induce transitions between states that differ no more than one in M_S and this is the origin of the $\Delta = |D| S_T^2$ relation. The derived energy-level diagram for **1** is shown in Figure 6, in which the states are labelled according to the expectation value of the cluster operator $\hat{S}_z$. Note that since the exchange coupling is dominated by the ferromagnetic Mn–Os Ising interaction, by labelling the states according to a total spin, S is not meaningful. From inspection of the

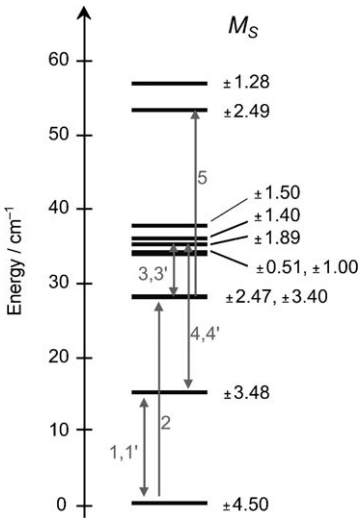

Figure 6. Energy-level diagram for **1**. Arrows indicate INS transitions that pertain to Figure 4.

energy-level diagram one might hope for a spin-reversal barrier of around 48 K ($\approx$34 cm^{-1}) instead of the 19 K established from the ac susceptibility measurements. The energy scheme does not allow for spin–phonon relaxation and was calculated in the approximation of a rigid lattice. The extracted dependency of the relaxation time on the temperature accounts for the spin–phonon coupling interaction and, therefore, the barriers determined from the energy-level diagram and from ac susceptibility measurements differ. The very factors that lead to the large Ising exchange—namely, the more diffuse valence orbitals and larger spin–orbit coupling—also facilitate an efficient interaction between the electron spins and the phonon bath. Moreover, although the differences in the orientation of the *z*-axes of the Mn^{III} zero-field splitting tensor and the Os^{III}–Mn^{III} superexchange interaction is not large enough to produce a notable effect on the energy pattern and related dc susceptibility and INS data, the misaligned axes will give rise to an additional transverse term that accelerates the quantum tunnelling of magnetisation and so reduces the height of the spin-reversal barrier.

Conclusion

In summary, the effect of substituting a 3d ion with a 5d ion of the same group on the SMM properties of a cyanide-based cluster has been illuminated by a spectroscopic and magnetic study of the two isostructural compounds, (NEt_4)-$[Mn_2(5\text{-Brsalen})_2(MeOH)_2M(CN)_6]$ with M = Os, Fe. Replacing $[Fe(CN)_6]^{3-}$ by $[Os(CN)_6]^{3-}$ leads to larger, more anisotropic exchange interactions and a distinct increase in the blocking temperature. We conclude that anisotropic exchange interactions are a promising source of introducing magnetic anisotropy in SMM, which has traditionally been achieved by uni-axial zero-field splittings.

Experimental Section

All chemicals and solvents used for the syntheses were of reagent grade.

Starting materials: $[Mn(5\text{-Brsalen})(H_2O)]PF_6$ was prepared by mixing $Mn_3O(CH_3COO)_7{\cdot}2H_2O$ with 5-BrsalenH_2[40] and NH_4PF_6 in methanol in the relative molar amounts 1:1:1.5 followed by slow evaporation of the solvent. $(PPh_4)_3[Os(CN)_6]$ and $(NEt_4)_3[Fe(CN)_6]$ were synthesised as described in the literature.[27,41]

Synthesis of 1: A solution of $(PPh_4)_3[Os(CN)_6]$ (680 mg, 0.5 mmol) in methanol (50 mL) was stirred with NEt_4ClO_4 (160 mg, 0.7 mmol) for 20 min and the solution was filtered and added to a solution of $[Mn(5\text{-Brsalen})(H_2O)]PF_6$ (330 mg, 0.5 mmol) in methanol (150 mL) without stirring. The resulting solution was kept in the dark for 1 d to yield dark brown crystals suitable for single-crystal X-ray diffraction. The crystals were kept in contact with the mother liquor to prevent deterioration. Yield: >80%; elemental analysis calcd (%) for $C_{48}H_{52}Br_4OsMn_2N_{11}O_6$: C 38.4, N 10.3, H 3.5; found: C 38.0, N 10.3, H 3.2.

Synthesis of 2: A solution of $(NEt_4)_3[Fe(CN)_6]$ (300 mg, 0.5 mmol) in methanol (50 mL) was added to a solution of $[Mn(5\text{-Brsalen})(H_2O)]PF_6$ (330 mg, 0.5 mmol) in methanol (150 mL) without stirring. The resulting solution was kept in the dark for 1 d to yield dark brown crystals suitable for single crystal X-ray diffraction. The crystals were kept in contact with the mother liquor to prevent deterioration. Yield: >80%; elemental analysis calcd (%) for $C_{48}H_{52}Br_4FeMn_2N_{11}O_6$: C 42.2, N 11.3, H 3.8; found: C 41.8, N 11.1, H 3.7.

X-ray crystallography: Single-crystal X-ray diffraction data were collected at 122 K using a Nonius Kappa CCD area-detector diffractometer with $Mo_{K\alpha}$ radiation (wavelength = 0.71073 Å) equipped with an Oxford Cryostreams low-temperature device. The structures were solved using direct methods (SHELXS97) and refined using the SHELXL97 software package.[42] All non-hydrogen atoms were refined anisotropically, whereas hydrogen atoms were fixed.

CCDC-755220 (**1**) and -755221 (**2**) contain the supplementary crystallographic data for this paper. These data can be obtained free of charge from The Cambridge Crystallographic Data Centre via www.ccdc.cam.ac.uk/data_request/cif.

Susceptibility measurements: All susceptibility measurements were carried out using Quantum-Design™ MPMS-XL SQUID magnetometers located at the University of Berne in Switzerland or at the University of Copenhagen. The sample ($\approx$10–20 mg) was wrapped in polyethylene film and placed in the middle of a standard SQUID straw. Measurements were conducted at fields of 1000 and 5000 Oe. The susceptibility was corrected for diamagnetic contributions by means of Pascal constants. Ac susceptibility measurements were measured with various frequencies in the range 1–1500 Hz with an ac field amplitude of 3 Oe without any applied static field.

Inelastic neutron scattering: INS studies of **1** were carried out using the direct-geometry time-of-flight neutron spectrometer IN5 located at the Institut Laue-Langevin, Grenoble, France. Crystalline **1** (ca. 2 g) was loaded into a 10 mm-diameter double-wall hollow aluminium measurement cylinder. All experiments utilised a standard ILL Orange cryostat for temperature control. The background was determined by measuring an empty aluminium sample holder and the spectrum subtracted from that of the sample. The detector efficiency correction was performed using data collected from vanadium. The wavelength of the incident neutrons was 3.8 and 4.0 Å and spectra were obtained at temperatures 1.5 and 15 K. The data were reduced and analysed using the DAVE (Data Analysis and Visualization Environment) program package.[43]

Acknowledgements

A.V.P., S.I.K., S.O. and O.S.R. thank the Swiss National Science Foundation (grant no. IZ73ZO-128078/1) and the Supreme Council for Science and Technological Development of Moldova for financial support. Prof. Silvio Decurtins (University of Berne) is thanked for the use of the SQUID magnetometer. K.S.P. thanks the Danish Neutron Scattering Society (DANSCATT) and the Danish Chemical Society for financial support.

[1] G. S. Girolami, W. R. Entley, *Science* **1995**, *268*, 397–400.
[2] D. Gatteschi, R. Sessoli, *Angew. Chem.* **2003**, *115*, 278–309; *Angew. Chem. Int. Ed.* **2003**, *42*, 268–297.
[3] R. Sessoli, D. Gatteschi, A. Caneschi, M. A. Novak, *Nature* **1993**, *365*, 141–143.
[4] M. N. Leuenberger, D. Loss, *Nature* **2001**, *410*, 789–793.
[5] O. Waldmann, *Inorg. Chem.* **2007**, *46*, 10035–10037.
[6] C. P. Berlinguette, D. Vaughn, C. Cañada-Vilalta, J.-R. Galán-Mascarós, K. R. Dunbar, *Angew. Chem.* **2003**, *115*, 1561–1564; *Angew. Chem. Int. Ed.* **2003**, *42*, 1523–1526.
[7] A. V. Palii, S. M. Ostrovsky, S. I. Klokishner, B. S. Tsukerblat, C. S. Berlinguette, K. R. Dunbar, J. R. Galan-Mascaros, *J. Am. Chem. Soc.* **2004**, *126*, 16860–16867.
[8] B. S. Tsukerblat, A. V. Palii, S. M. Ostrovsky, S. V. Kunitsky, S. I. Klokishner, K. R. Dunbar, *J. Chem. Theory Comput.* **2005**, *1*, 668–673.
[9] A. V. Palii, S. M. Ostrovsky, S. I. Klokishner, B. S. Tsukerblat, K. R. Dunbar, *ChemPhysChem* **2006**, *7*, 871–879.
[10] M. Atanasov, C. Busche, F. El Hallah, B. Martin, G. Rajaraman, J. van Slageren, H. Wadepohl, *Inorg. Chem.* **2008**, *47*, 8112–8125.
[11] N. Ishikawa, M. Sugita, T. Ishikawa, S. Koshihara, Y. Kaizu, *J. Am. Chem. Soc.* **2003**, *125*, 8694–8695.
[12] N. Ishikawa, M. Sugita, T. Ishikawa, S. Koshihara, Y. Kaizu, *J. Phys. Chem. B* **2004**, *108*, 11265–11271.
[13] N. Ishikawa, M. Sugita, W. Wernsdorfer, *J. Am. Chem. Soc.* **2005**, *127*, 3650–3651.
[14] N. Ishikawa, M. Sugita, W. Wernsdorfer, *Angew. Chem.* **2005**, *117*, 2991–2995; *Angew. Chem. Int. Ed.* **2005**, *44*, 2931–2935.
[15] M. A. AlDamen, J. M. Clemente-Juan, E. Coronado, C. Martí-Gastaldo, A. Gaita-Ariño, *J. Am. Chem. Soc.* **2008**, *130*, 8874–8875.
[16] M. A. AlDamen, S. Cordona-Serra, J. M. Clemente-Juan, E. Coronado, A. Gaita-Arino, C. Marti-Gastaldo, F. Luis, O. Montero, *Inorg. Chem.* **2009**, *48*, 3467–3479.
[17] S. Osa, T. Kido, N. Matsumoto, N. Re, A. Pochaba, J. Mrozinski, *J. Am. Chem. Soc.* **2004**, *126*, 420–421.
[18] S. I. Klokishner, S. M. Ostrovsky, O. S. Reu, A. V. Palii, P. L. W. Tregenna-Piggott, T. Brock-Nannestad, J. Bendix, H. Mutka, *J. Phys. Chem. C* **2009**, *113*, 8573–8582.
[19] J. Bendix, P. Steenberg, I. Søtofte, *Inorg. Chem.* **2003**, *42*, 4510–4512.
[20] E. J. Schelter, A. V. Prosvirin, K. R. Dunbar, *J. Am. Chem. Soc.* **2004**, *126*, 15004–15005.
[21] A. V. Palii, S. M. Ostrovsky, S. I. Klokishner, B. Tsukerblat, E. J. Schelter, A. V. Prosvirin, K. R. Dunbar, *Inorg. Chim. Acta* **2007**, *360*, 3915- 3923.
[22] E. J. Schelter, F. Karadas, C. Avendano, A. V. Prosvirin, W. Wernsdorfer, K. R. Dunbar, *J. Am. Chem. Soc.* **2007**, *129*, 8139–8149.
[23] D. E. Freedman, D. M. Jenkins, A. T. Iavarone, J. R. Long, *J. Am. Chem. Soc.* **2008**, *130*, 2884–2885.
[24] Y. Song, P. Zhang, X.-M. Ren, X.-F. Shen, Y.-Z. Li, X.-Z. You, *J. Am. Chem. Soc.* **2005**, *127*, 3708–3709.
[25] J. H. Yoon, J. H. Lim, H. C. Kim, C. S. Hong, *Inorg. Chem.* **2006**, *45*, 9613–9615.
[26] J. J. Sokol, A. G. Hee, J. R. Long, *J. Am. Chem. Soc.* **2002**, *124*, 7656–7657.
[27] P. Albores, L. P. Slep, L. M. Baraldo, R. Baggio, M. T. Garland, E. Rentschler, *Inorg. Chem.* **2006**, *45*, 2361–2363.
[28] V. S. Mironov, *Dokl. Phys. Chem.* **2007**, *415*, 199–204.
[29] M. Hilfiger, M. Shatruk, A. Prosvirin, K. R. Dunbar, *Chem. Commun.* **2008**, *44*, 5752–5754.
[30] M. G. Hilfiger, M. Chen, T. V. Brinzari, T. M. Nocera, M. Shatruk, D. T. Petasis, J. L. Musfeldt, C. Achim, K. R. Dunbar, *Angew. Chem.* **2010**, *122*, 1410–1413.
[31] A. V. Palii, O. S. Reu, S. M. Ostrovsky, S. I. Klokishner, B. Tsukerblat, M. Hilfiger, M. Shatruk, A. Prosvirin, K. R. Dunbar, *J. Phys. Chem. A* **2009**, *113*, 6886–6890.
[32] H. Miyasaka, N. Matsumoto, H. Ōkawa, N. Re, E. Gallo, C. Floriani, *J. Am. Chem. Soc.* **1996**, *118*, 981–994.
[33] H. J. Choi, J. J. Sokol, J. R. Long, *Inorg. Chem.* **2004**, *43*, 1606–1608.
[34] P. L. W. Tregenna-Piggott, D. Sheptyakov, L. Keller, S. I. Klokishner, S. M. Ostrovsky, A. V. Palii, O. S. Reu, J. Bendix, T. Brock-Nannestad, K. Pedersen, H. Weihe, H. Mutka, *Inorg. Chem.* **2009**, *48*, 128–134.
[35] M. Ferbinteanu, H. Miyasaka, W. Wernsdorfer, K. Nakata, K.-i. Sugiura, M. M. Yamashita, C. Coulon, R. Clérac, *J. Am. Chem. Soc.* **2005**, *127*, 3090–3099.
[36] J. S. Griffith, *The Theory of Transition-Metal Ions*, Cambridge University Press, Cambridge, **1961**, p. 365.
[37] P. L. W. Tregenna-Piggott, Available in the DAVE program suite.
[38] Q. Scheifele, C. Riplinger, F. Neese, H. Weihe, A.-L. Barra, F. Juranyi, A. Podlesnyak, P. L. W. Tregenna-Piggott, *Inorg. Chem.* **2008**, *47*, 439–447.
[39] J. Villain, F. Hartman-Boutron, R. Sessoli, A. Rettori, *Europhys. Lett.* **1994**, *27*, 159.
[40] Prepared by condensation of 2 equiv 5-bromosalicylic aldehyde with 1 equiv ethylenediamine in hot methanol.
[41] P. Mascharak, *Inorg. Chem.* **1986**, *25*, 245–247.
[42] G. M. Sheldrick, *Acta Crystallogr.* **2008**, ##*A64*, 112–122.
[43] R. Azuah, J. Copley, R. Dimeo, S. Park, S.-H. Lee, A. Munter, L. Kneller, Y. Qiu, I. Peral, C. Brown, P. Kienzle, P. L. W. Tregenna-Piggott, Dave 1.4 Beta. (http://www.ncnr.nist.gov/dave).

Received: May 10, 2010
Published online: October 11, 2010

